

Superscripts

| | |
|-----------|-------------------------|
| <i>T</i> | = for the core region |
| <i>sc</i> | = for the screen region |
| <i>B</i> | = for the bed region |

Subscripts

| | |
|----------|------------------------|
| <i>o</i> | = at the reactor inlet |
|----------|------------------------|

LITERATURE CITED

- Ahmed, M. and R. W. Fahien, "Tubular Reactor Design—I. Two Dimensional Model," *Chem. Eng. Sci.*, **35**, 889 (1980).
- Argo, W. B. and J. M. Smith, "Heat Transfer in Packed Beds," *Chem. Eng. Prog.*, **49**, 443 (1953).
- Ascher, U., J. Christiansen, and R. D. Russell, "COLSYS—A Collocation Code for Boundary Value Problems," Proceedings of Working Conference for Codes for Boundary Value Problems in ODE's, Houston, TX (May, 1978).
- Carberry, J. J., *Chemical and Catalytic Reaction Engineering*, McGraw-Hill, New York (1976).
- Dalla Betta, R. A., A. G. Piken, and M. J. Shelef, "Heterogeneous Methanation: Steady-State CO Hydrogenation on Supported Ruthenium, Nickel, and Rhodium," *J. of Catal.*, **40**, 173 (1975).
- Davis, M. E., G. Fairweather, and J. Yamanis, "Annular Bed Reactor—Methanation of Carbon Dioxide," *Can. J. Chem. Eng.*, **59**, 497 (1981).
- Davis, M. E., "Analysis of an Annular Bed Reactor for the Methanation of Carbon Oxides," Ph.D. Thesis, University of Kentucky, Lexington, Kentucky (1981).
- DeBruijn, E. W., W. A. DeJong, and T. VanDerSpeigel, "Methanation in a Parallel Passage Reactor," *ACS Symp. Ser.*, No. 65, 63 (1978).
- DeWasch, A. P. and G. Froment, "Heat Transfer in Packed Beds," *Chem. Eng. Sci.*, **27**, 567 (1972).
- Eckert, E. R. G. and R. M. Drake, *Heat and Mass Transfer*, McGraw-Hill, New York (1959).
- Fahien, R. W. and J. M. Smith, "Mass Transfer in Packed Beds," *AIChE J.*, **1**, 28 (1955).
- Fahien, R. W. and I. M. Stankovic, "An Equation for the Velocity Profile in Packed Columns," *Chem. Eng. Sci.*, **34**, 1350 (1979).
- Fand, R. M., "Heat Transfer by Forced Convection from a Cylinder to Water in Crossflow," *Int. J. Heat Mass Transfer*, **8**, 995 (1965).
- Goodman, D. W., R. D. Kelly, T. E. Madey, and J. T. Yates, "Kinetics of the Hydrogenation of CO over a Single Crystal Nickel Catalyst," *J. of Catal.*, **44**, 226 (1980).
- Haynes, W. P., R. R. Schehl, J. K. Weber, and A. J. Forney, "The Study of an Adiabatic Parallel Plate Methanation Reactor," *Ind. Eng. Chem. Proc. Des. Dev.*, **16**, 113 (1977).
- Jarvi, G. A., K. B. Mayo, and C. H. Bartholomew, "Monolithic-Supported Nickel Catalysts: I. Methanation Activity Relative to Pellet Catalysts," *Chem. Eng. Commun.*, **4**, 325 (1980).
- Lawson, J. D. and J. L. Morris, "The Extrapolation of First Order Methods for Parabolic Partial Differential Equations. I," *SIAM J. Numer. Anal.*, **15**, 1212 (1978).
- Lindberg, B., "On Smoothing and Extrapolation for the Trapezoidal Rule," *B.I.T.*, **11**, 29 (1971).
- Mehta, D. and M. C. Hawley, "Wall Effect in Packed Columns," *Ind. Eng. Chem. Proc. Des. Dev.*, **8**, 280 (1969).
- Penline, H. W., R. R. Schehl, and W. P. Haynes, "Operation of a Tube Wall Methanation Reactor," *Ind. Eng. Chem. Proc. Des. Dev.*, **18**, 56 (1979).
- Satterfield, C. N., *Mass Transfer in Heterogeneous Catalysis*, M.I.T. Press, Cambridge (1970).
- Schuler, R. W., V. P. Stallings, and J. M. Smith, "Heat and Mass Transfer in Fixed-Bed Reactors," *CEP Symp. Ser.*, **48**(4), 28 (1952).
- Schertz, W. W. and K. B. Bischoff, "Thermal and Material Transport in Nonisothermal Packed Beds," *AIChE J.*, **15**, 597 (1969).
- Schwartz, C. E. and J. M. Smith, "Flow Distribution in Packed Beds," *Ind. Eng. Chem.*, **45**, 1209 (1953).
- Shah, M. A. and D. Roberts, "Mass Transfer Characteristics of Stacked Metal Screens," *Adv. Chem. Ser.*, **133**, 259 (1974).
- Vannice, M. A., "The Catalytic Synthesis of Hydrocarbons from H₂/CO Mixtures over the Group VIII Metals—IV. The Kinetics Behavior of CO Hydrogenation over Ni Catalysts," *J. of Catal.*, **44**, 152 (1976).

Manuscript received January 23, 1981; revision received April 30, and accepted May 15, 1981

Diffusional Influences on Deactivation Rates: Experimental Verification

The internal diffusion-deactivation model of Krishnaswamy and Kittrell (1981a) is tested and verified by using laboratory deactivation data on the decomposition of hydrogen peroxide by immobilized catalase. Through an analysis of the influence of diffusional phenomena on the deactivation kinetics, estimates of the intrinsic deactivation rate constant have also been provided.

S. KRISHNASWAMY

and

J. R. KITTRELL

Department of Chemical Engineering
University of Massachusetts
Amherst, MA 01003

SCOPE

Deactivation effects can be masked by diffusion in catalyst particles leading to erroneous measurements of deactivation rate constants from laboratory data. Effective measurements of intrinsic deactivation rate constants are, however, required for development of generalized theories of deactivation and reactor design. Computer solutions have been developed for a few problems in this category, but the solutions are so complex

that they have not been generally applied to experimental deactivation data.

In a recent theoretical study, Krishnaswamy and Kittrell (1981) developed a model descriptive of deactivation data exhibiting the masking effects of internal diffusion, for the case of first order reaction with first order concentration-independent deactivation. The present experimental study was undertaken to examine the applicability of the model to deactivation data. For this purpose, data taken on the decomposition of hydrogen peroxide by immobilized catalase were used to test the theoretical developments.

S. Krishnaswamy is with Gulf Research & Development Co.; Harnarville, PA.
0001-1541/82-0254-0273-\$2.00 © The American Institute of Chemical Engineers, 1982.

CONCLUSIONS AND SIGNIFICANCE

A preliminary test of the internal diffusion-deactivation model of Krishnaswamy and Kittrell (1981a) has been conducted using laboratory data on the decomposition of hydrogen peroxide by immobilized catalase. It has been shown that the model describes the data adequately over a wide range of internal diffusional limitations. The model predicts a single value of the

intrinsic deactivation rate constant that is suitable for all the experimental runs. Hence, for systems experiencing diffusion-limited, concentration-independent catalyst decay, estimates of intrinsic deactivation rate constants which are free from the masking effects of diffusion can be obtained.

INTRODUCTION

Most catalytic processes are afflicted by catalyst deactivation, whereby thermal degradation or deposition of feed poisons or coke causes the catalyst to lose its full activity. Indeed, the economic viability of commercial catalytic processes are often governed by the rate of this decay in catalyst activity. In catalytic cracking, hydrocracking, reforming and desulfurization operations, catalyst lifetimes from several hours to several years are observed. Ogunye and Ray (1971) have cited other examples of reactions of commercial importance which are plagued by catalyst deactivation.

Modeling of the kinetics of industrial reactions requires a variety of simplifying, but useful, approximations. For example, a broad spectrum of hydrocarbon compounds can be usefully represented by a single pseudo-compound in hydrocracking kinetic modeling (Stangeland and Kittrell, 1972). Similarly, industrial deactivation kinetics can often be approximated adequately by separable rate forms, wherein the rate of reaction is expressed by a product of temperature dependent, concentration dependent and time dependent (deactivation) terms (Szepe and Levenspiel, 1968). As such, the rate of decay of catalyst activity is often represented by a simple, concentration-independent rate form (Weekman and Nace, 1970).

A further complication in the modeling of many solid-catalyzed systems is the presence of significant mass transfer resistances. Furthermore, the effect of these mass transfer resistances on the deactivation process can appear in two broad categories. First, the decreasing relative diffusional resistance as the intrinsic activity of the catalyst diminishes will alter the apparent overall rate of conversion of reactants to products. As shown by Masamune and Smith (1966), diffusion may either extend or shorten the useful catalyst lifetime, relative to the diffusion-free case, depending upon the form of the kinetic expressions. Second, the deactivation process may further alter the intrinsic transport properties. For example, Butt et al. (1975) concluded in studies on hydrogen-mordenite that the effective diffusivity of the catalyst decreased by at least a factor of two during the coking process, and that it was nonlinearly related to catalyst coke level.

Several theoretical studies have addressed the modeling of deactivating systems involving significant diffusional resistances. In addition to those cited above, Wheeler (1955), Chu (1968), Olson (1968), Hegedus and Petersen (1973a) and Hegedus (1974) have attacked distinctive classes of problems of relevance to the topic. Representative experimental studies have been made by Balder and Petersen (1968), Hegedus and Petersen (1973b), and Suga et al. (1967).

Recently, Krishnaswamy and Kittrell (1981a, 1981b) have

developed analytical solutions for concentration-independent deactivation models involving both internal and external diffusional resistances. They have observed that, although the effectiveness factors thereby derived are inherently nonlinear, the Levenspiel plots (Levenspiel, 1972) are often approximately linear in the presence of diffusional resistance. Furthermore, the effectiveness factors exhibit strong analogies to the classical Thiele theory (Smith, 1970). An experimental confirmation of this theory is presented herein, using the decomposition of hydrogen peroxide by immobilized catalase in a plug flow reactor as a model system.

THEORETICAL SUMMARY

For a first order reaction in a single pellet, undergoing deactivation by a first order, concentration-independent loss of sites, the following mass balances are appropriate for relatively slow deactivation:

$$D_A \left(\frac{d^2 C_{Ar}}{dr^2} + \frac{2}{r} \frac{dC_{Ar}}{dr} \right) = k_i C_{Ar} a \quad (1)$$

$$-\frac{da}{dt} = k_d a \quad (2)$$

Defining an initialized deactivation effectiveness factor as the overall reaction rate at any time divided by the diffusion-free rate at zero time, Krishnaswamy and Kittrell (1981a) have shown that the initialized effectiveness factor becomes:

$$\eta_t = \frac{A}{h} (\text{Coth } \phi - 1/\phi) \quad (3)$$

where h is the classical Thiele modulus, ϕ is a deactivation modulus, and A is a deactivation time scale, respectively, given by:

$$h = \frac{R}{3} \sqrt{k_i/D_A}; \phi = 3hA; A = \exp(-k_d t/2) \quad (4)$$

For an isothermal plug flow reactor, the conversion-time relationship will follow that of a Levenspiel plot (Levenspiel, 1972):

$$\ln \ln (1/(1-x)) = \ln k\tau + \ln \eta_t \quad (5)$$

Although the initialized effectiveness factor of Eq. 5 is nonlinearly dependent upon time (through Eqs. 3 and 4), Krishnaswamy and Kittrell (1981a) have shown Eq. 5 to be exactly linear for conditions of negligible internal diffusion and extreme internal diffusion, as summarized in Table 1. As reported herein, the Levenspiel plots can also appear linear in the presence of experimental error for intermediate values of the deactivation modulus.

This theory has strong analogies to the classical Thiele theory (Smith, 1970), as summarized in Table 2. For the diffusion-free case, both the Arrhenius plot in the classical kinetic analysis and the Levenspiel plot in the deactivation analysis provide valid estimates of the intrinsic parameters. With severe internal diffusion, both plots exhibit slopes which are one-half the intrinsic value. With severe external diffusion, the Arrhenius slope approaches zero, except for the temperature dependence of the mass transfer coefficient; the Levenspiel slope also approaches zero. For both plots, the slope is a function of reciprocal particle radius for intermediate and high levels of internal diffusional resistance.

In the present study, the predictions of the deactivation analysis are verified by experimental investigations using immobilized catalase.

TABLE 1. LIMITING CASES FOR LEVENSPIEL PLOTS WITH INTERNAL DIFFUSION

$$\ln \ln \left(\frac{1}{1-x} \right) = \ln k_p \cdot \tau - k_{dp} \cdot t$$

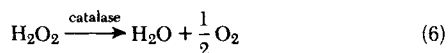
| Deactivation Modulus Terms | Pseudo-Reaction Rate Constant | Pseudo-Deactivation Rate Constant |
|----------------------------|---|---|
| $hA = 0$ | $k_p = k$ (true intrinsic constant) | $k_{dp} = k_d$ (true intrinsic constant) |
| $hA > 5$ | $k_p = k/h$ | $k_{dp} = k_d/2$ |
| $hA > 1$ | $k_p = k \left(\frac{1}{h} - \frac{1}{3h^2} \right)$ | $k_{dp} = k_d \left(\frac{1}{2} + \frac{1}{6hA} \right)$ |

TABLE 2. ANALOGOUS CHARACTERISTICS OF DIFFUSION FOR DEACTIVATING AND NONDEACTIVATING SYSTEMS

| Condition | Kinetic Analysis | Deactivation Analysis |
|--------------------------------------|-------------------------------------|---------------------------------------|
| Slope without diffusion | E | k_d |
| Slope with severe internal diffusion | $E/2$ | $k_d/2$ |
| Slope with severe external diffusion | $\rightarrow 0$ | $\rightarrow 0$ |
| Dependence on Particle Radius | $(k)_p = f\left(\frac{1}{R}\right)$ | $(k_d)_p = f\left(\frac{1}{R}\right)$ |

EXPERIMENTAL

The enzyme catalase converts hydrogen peroxide into water and oxygen according to the following reaction:



Catalase can be used industrially to remove hydrogen peroxide, for example in the pasteurization of milk. Coupled with glucose oxidase, the multienzyme system also has possible applications in the food and medicinal industry.

The reasons for the choice of this model system are multiple. Catalase and its substrate, hydrogen peroxide, are available commercially and inexpensively. The system is simple and the reaction takes place under very mild conditions. The time-scale of decay of immobilized catalase is very convenient for conducting laboratory experiments. The progress of the reaction can be followed easily either by measuring the amount of oxygen in the reactor effluent, or by titrating feed and effluent samples to determine peroxide levels. The theoretical model of Krishnaswamy and Kittrell (1981a) assumes first order kinetics for the main reaction and deactivation. The catalase system, when undergoing thermal deactivation, would apparently deactivate in accordance with these kinetics. Hence it is a logical choice of an experimental system to validate the theoretical model. Another major advantage of such an immobilized enzyme system is that the active sites are known and can be measured in spent catalysts. Furthermore, the nature and size of supports, upon which the enzyme is immobilized, can be varied to achieve experimental conditions required for verification of the theory.

Altomare (1974a, b) studied the deactivation of catalase in a tubular flow reactor. By developing a simple analytical model to predict peroxide concentration and immobilized catalase activity as a function of time and position, he has also shown that peroxide decomposition and catalase deactivation by peroxide follow apparent first order kinetics in the range of 0.1 M to 0.001 M peroxide.

Altomare has also shown that decomposition and deactivation rates increase with increasing temperature for this system. The temperature effects were more pronounced on enzyme deactivation than peroxide decomposition. In fact, at temperatures above ambient and low feed peroxide concentrations (below 0.001 M), a thermal deactivation mechanism will be predominant. The deactivation of the enzyme then can be described by Eq. 2. The use of fungal catalase for this study, rather than the more peroxide-sensitive beef-liver catalase (Altomare, 1974b), further ensures that the deactivation kinetics will match those of the theoretical development.

Materials

For this research work, fungal catalase was purchased from Searle Biochemicals. The soluble enzyme had an activity of 240,000 IU/g and a molecular weight of approximately 200,000 to 250,000. The support used was Eagle Picher natural Kieselguhr, Celaton MP-76 and MP-91. The supports were crushed and sieved to yield the required particle sizes.

Methods of Immobilization

Prior to immobilization, the support was washed and dried. Then the support was sieved and silanized, by placing it in a round bottom flask along with a 10% solution (by volume) of γ -amino propyl-triethoxysilane (γ -APTES) and toluene. After refluxing the mixture for approximately 24 hours, the support was washed with toluene five times to remove γ -APTES. Then it was washed with acetone to remove the toluene, and dried.

Then, 25 mL of 2.5% aqueous glutaraldehyde was added to 10 g of silanized support for the coupling reaction. The support and solution were allowed to react for 90 minutes, at room temperature, with intermittent stirring. After decanting the glutaraldehyde, the support was washed five times with distilled water to remove traces of glutaraldehyde. Meanwhile, an enzyme solution was prepared by dissolving 200 mg of the soluble cat-

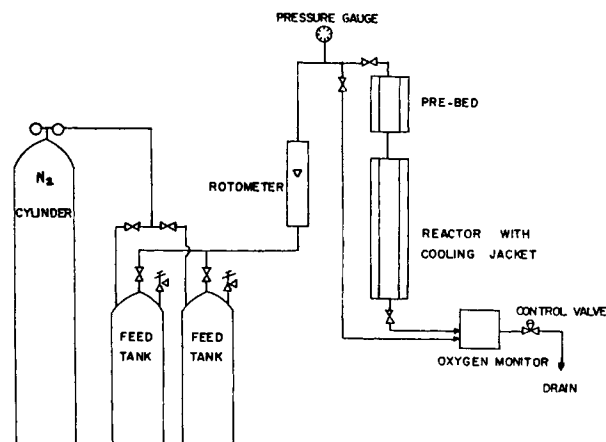


Figure 1. Schematic of reactor system.

alase in 15 mL of citrate-phosphate buffer of pH 7.5. As soon as the activated support was prepared, the enzyme solution was added and the enzyme coupling reaction carried out for 60 minutes, at ambient temperature with intermittent stirring. After 60 minutes, the support was repeatedly washed with the citrate-phosphate buffer to remove any uncoupled soluble enzyme. The immobilized enzyme was then stored in pH 7.0 buffer at 5°C. The enzyme concentration in the immobilizing solution was very high and it was assumed that one hour was sufficient time to allow for diffusion of the enzyme and its uniform distribution inside the particle.

In order to provide a wide range of effectiveness factors, selected catalysts were exposed to elevated temperatures, thereby reducing their intrinsic activity (Krishnaswamy, 1978).

Reactor Tests

A schematic diagram of the equipment used for the flow reactor tests is shown in Figure 1. A glass reactor of 10.0 mm diameter was placed in series with feed tanks, flowmeter, and a Beckman oxygen analyzer. A pre-bed filled with the support material was placed in series with the reactor, in order to filter out any particles in the feed and to ensure that the support did not contribute to the reaction. The feed was metered to the reactor under pressure and flow was controlled by means of a control valve and the flowmeter. A bypass line allowed the measurement of peroxide concentration in the feed. The reactor had a jacket to allow liquid from a constant temperature bath to be circulated around the bed. Temperature was controlled to be at approximately 52°C for all the runs, by passing the feed line through a constant temperature bath and by circulating heat transfer fluid through the jacketed reactor. A feed peroxide concentration of 0.5×10^{-3} M was used for all the experiments in order to ensure concentration-independent deactivation, verified by separate tests (Krishnaswamy, 1978). The pH was maintained at 7.0 using a citrate-phosphate buffer.

Hydrogen peroxide levels were measured periodically at reactor inlet and outlet using the standard iodometric titration procedure. The feed solution was sparged with nitrogen to remove traces of oxygen. Prior to the commencement of each run, the immobilized enzyme was packed in the reactor and distilled deionized water was passed over it for 12 hours. This was to ensure that any unattached enzyme present on the support particles was removed.

Film diffusional resistances are believed to be unimportant, as discussed in detail elsewhere (Krishnaswamy, 1978).

EXPERIMENTAL RESULTS

The conditions under which six experiments, with varying degrees of internal diffusional limitations, were performed are listed in Table 3. Conversion-time data for the six experimental runs are presented in Table 4. Figure 2 is a representative plot of the percent conversion of hydrogen peroxide in the feed with time, showing how the conversion decreased as the enzyme deactivated during the time span of the experiment. By extrapolating the conversion versus time graphs to zero time, apparent first order rate constants were calculated, assuming first order peroxide decomposition kinetics and plug flow of fluid (Table 3).

To estimate the kinetic effectiveness factor, it was assumed that

TABLE 3. EXPERIMENTAL RUN CONDITIONS AND ESTIMATED PARAMETERS

| Run No. | Experimental Variables | | Estimated Values | | | | |
|---------|--|-------------|-------------------|--------------------------------|--------------------------|-------|--------|
| | $\tau \left(\frac{\text{g s}}{\text{mL}} \right)$ | $d_p (\mu)$ | k_p (ml/g s) | k_{dp} (h ⁻¹) | k_i (s ⁻¹) | h | η |
| A | 1.50 | 841-1,000 | 2.1 | 0.26 | 35.5 | 40.0 | 0.025 |
| B | 4.56 | 1,200-1,700 | 0.187 | 0.275 | 0.90 | 10.25 | 0.098 |
| C | 4.94 | 841-1,000 | 0.358 | 0.343 | 1.07 | 6.94 | 0.144 |
| D | 5.00 | 420-595 | 0.395 | 0.345 | 0.37 | 2.07 | 0.405 |
| E | 4.10 | 300-420 | 0.386 | 0.379 | 0.255 | 1.317 | 0.565 |
| F | 4.10 | 420-595 | 0.184 | 0.42 | 0.081 | 0.967 | 0.680 |

TABLE 4. EXPERIMENTAL CONVERSION VS. TIME DATA

| Run A | | Run C | | Run E | |
|-------------------------|--------------------------|-------------------------|--------------------------|-------------------------|--------------------------|
| Elapsed Time (hours) | Fractional Conversion | Elapsed Time (hours) | Fractional Conversion | Elapsed Time (hours) | Fractional Conversion |
| 0.0 | 0.93 | 0.25 | 0.81 | 0 | 0.795 |
| 1.0 | 0.90 | 1.0 | 0.70 | 1.25 | 0.635 |
| 2.0 | 0.83 | 2.0 | 0.576 | 2.0 | 0.510 |
| 4.0 | 0.684 | 3.0 | 0.445 | 3.0 | 0.397 |
| 5.75 | 0.51 | 4.0 | 0.37 | 4.25 | 0.255 |
| 7.0 | 0.42 | 5.0 | 0.273 | 5.0 | 0.22 |
| 8.75 | 0.26 | 6.0 | 0.204 | 6.0 | 0.15 |
| 10.0 | 0.20 | 7.0 | 0.15 | 7.0 | 0.104 |
| 11.0 | 0.16 | | | | |
| 12.5 | 0.11 | | | | |

| Run B | | Run D | | Run F | |
|-------------------------|--------------------------|-------------------------|--------------------------|-------------------------|--------------------------|
| Elapsed Time (hours) | Fractional Conversion | Elapsed Time (hours) | Fractional Conversion | Elapsed Time (hours) | Fractional Conversion |
| 0.25 | 0.57 | 0.25 | 0.840 | 0.0 | 0.545 |
| 1.0 | 0.475 | 1.0 | 0.750 | 1.0 | 0.370 |
| 2.0 | 0.39 | 2.0 | 0.620 | 2.0 | 0.29 |
| 3.0 | 0.30 | 3.0 | 0.484 | 3.0 | 0.183 |
| 4.0 | 0.23 | 4.0 | 0.40 | 4.25 | 0.13 |
| 5.0 | 0.186 | 5.0 | 0.29 | 5.0 | 0.08 |
| 6.0 | 0.14 | 6.0 | 0.22 | | |
| 7.0 | 0.115 | 7.0 | 0.167 | | |

the particles were spherical in shape with a diameter equal to the average of the range reported in Table 3. The effective diffusivity of peroxide was estimated to be $5.0 \times 10^{-6} \text{ cm}^2/\text{s}$ from values of the bulk diffusivity and properties of the support (Krishnaswamy, 1978). Effectiveness factors and intrinsic rate constants for the primary reaction were calculated by the method used by Rovito and Kittrell (1973) for immobilized glucose oxidase. The wide variation in the intrinsic rate constant of Table 3 is due to the preliminary inactivation discussed above, in order to achieve a wider variation in effectiveness factors than possible from particle size changes alone.

Levenspiel plots were made for all six runs, four of which are shown in Figure 3. Note that, even though the theory of Equation 5 would suggest nonlinearities, all of the plots appear linear within experimental accuracy as expected (Krishnaswamy and Kittrell, 1981a). Note that the slopes of these plots increase with increasing

values of the kinetic effectiveness factor, as expected by the theory. The intercepts do not rank in accordance with the effectiveness factor due to the variation of intrinsic activities and particle diameters. The slopes of Figure 3 represent the pseudo-deactivation rate constant, and are reported for all runs in Table 3.

PERFORMANCE OF DEACTIVATION-DIFFUSION MODEL

In order to estimate the magnitude of the intrinsic deactivation rate constant from these data, the following relationship could be considered (Table 1), which is valid only for $hA > 1.0$:

$$k_{dp} = k_d \left[\frac{1}{2} + \frac{1}{6hA} \right] \quad (7)$$

Although this relationship is difficult to utilize directly in analyzing experimental data, it does correctly suggest that the slopes of the Levenspiel plots (Figure 3) should approach $k_d/2$ as $1/h$ approaches zero. The exact plot of Eq. 5 has been shown to exhibit similar characteristics. The slopes of the Levenspiel plots versus their reciprocal Thiele moduli for the data of Tables 3 and 4 are presented in Figure 4.

The intercept of Figure 4 provides an estimate of $k_d/2$, the resulting intrinsic deactivation rate constant being 0.51 h^{-1} . Sums of squares contours on conversion using Eqs. 3 and 5 for each individual run were also plotted to confirm this estimate of k_d . As illustrated in Figure 5 for Run A, $k_d = 0.51 \text{ h}^{-1}$ does fall within the 90% confidence contour (see Kittrell, 1970, for calculational details), which ranges between 0.46 and 0.52 h^{-1} . Also, the independent estimate of the intrinsic kinetic rate constant for peroxide decomposition from Table 3 falls within the 90% contour of Figure 5.

Similar evaluations of the 90% confidence contour for the other experimental runs showed that $k_d = 0.51 \text{ h}^{-1}$ in Eqs. 3 and 5 adequately described all the data, except for Run C which required

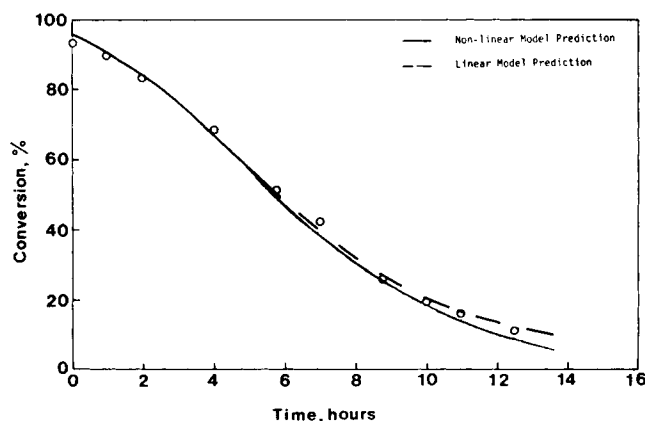


Figure 2. Illustrative deactivation of immobilized catalase (Run A).

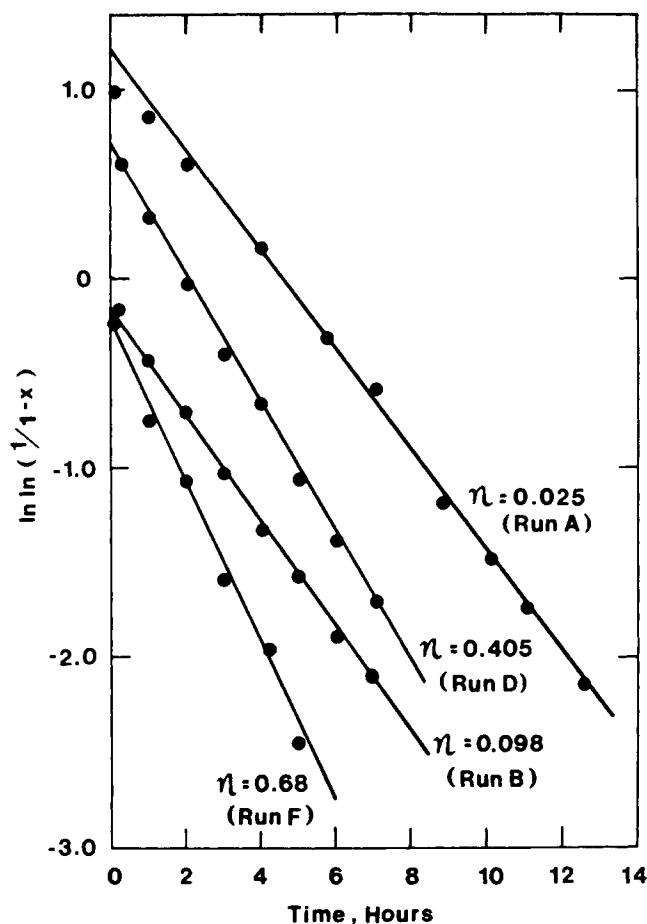


Figure 3. Representative Levenspiel plots.

a 10% higher value for k_d .

In Figure 6 is shown the predicted and observed conversions for all the data points of Table 4, using a value of $k_d = 0.51 \text{ h}^{-1}$ in Eqs. 3 and 5. The ability of the model to describe all of these data simultaneously, for kinetic effectiveness factors ranging from 0.02 to 0.68, is quite good. Only Run C exhibits consistent errors between predicted and observed values, for reasons discussed above.

The solid line of Figure 2 shows the agreement of this theoretical prediction for Run A (using $k_d = 0.51 \text{ h}^{-1}$ which is valid for all runs) with the experimental data. Also shown in Figure 2 is a dashed line, which represents the replotting of the linear line from Figure 3. Obviously, even though the theory of Eqs. 3 and 5 suggests the Levenspiel plots should be nonlinear, they are linear, whether viewed from the perspective of Figure 2 or Figure 3. Krishnaswamy (1978) has performed a Taylor expansion of Equation 5 and evaluated errors due to higher order terms.

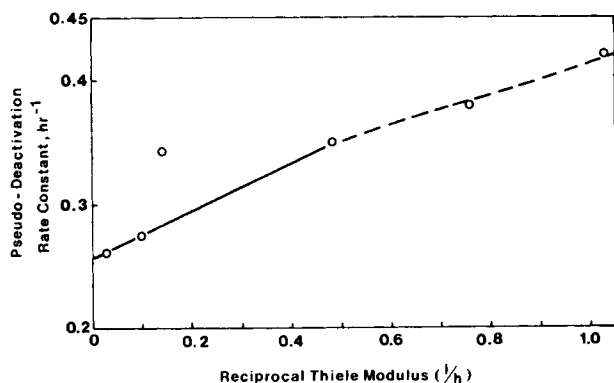


Figure 4. Pseudo deactivation rate constant dependence on Thiele modulus.

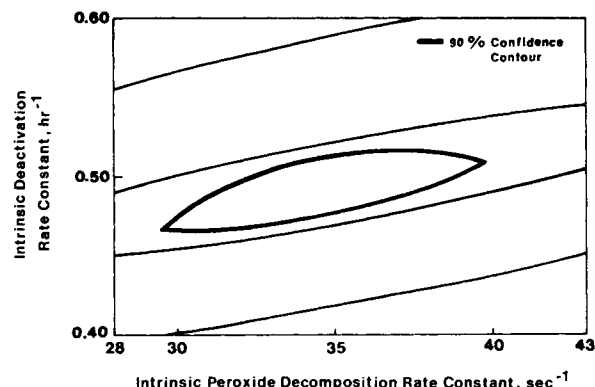


Figure 5. Illustrative sum of squares contours for Run A.

Based upon the observed linear behavior of the data of Figure 3, it would be expected that the last term in Eq. 5 could be expanded in a Taylor series, keeping only the first order term, to provide the following approximation:

$$\ln \ln \left(\frac{1}{1-x} \right) = \ln k \tau \eta - k_d \eta_d t \quad (8)$$

where:

$$\eta_d = \frac{\phi_o}{2} \left[\frac{1}{(\text{Coth } \phi_o - 1/\phi_o)} - \text{Coth } \phi_o \right] \quad (9)$$

Here, the deactivation modulus, ϕ , is evaluated at some arbitrary time t_o used in the Taylor expansion. Based upon the data of Figure 3, it appears that η_d is a constant within each experimental run. If it were possible to obtain a value of t_o by empirical curve fitting which also requires the relationship of η_d between runs to be governed by Eq. 9, the relationship of Eqs. 8 and 9 would be equivalent to that of Eqs. 3 and 5, within observed experimental error.

If we accept the intrinsic deactivation rate constant to be 0.51 h^{-1} , the ratio of the measured pseudo-deactivation rate constant (slope of the Levenspiel plots) to this intrinsic constant becomes experimental estimates of η_d (Eq. 8). These experimental values of η_d are plotted in Figure 7. A value of $t_o = 2 \text{ h.}$ was found which provides the theoretical η_d vs. h curve from Eq. 9, shown as the solid line in Figure 7.

The experimental points shown in Figure 7 are in close agree-

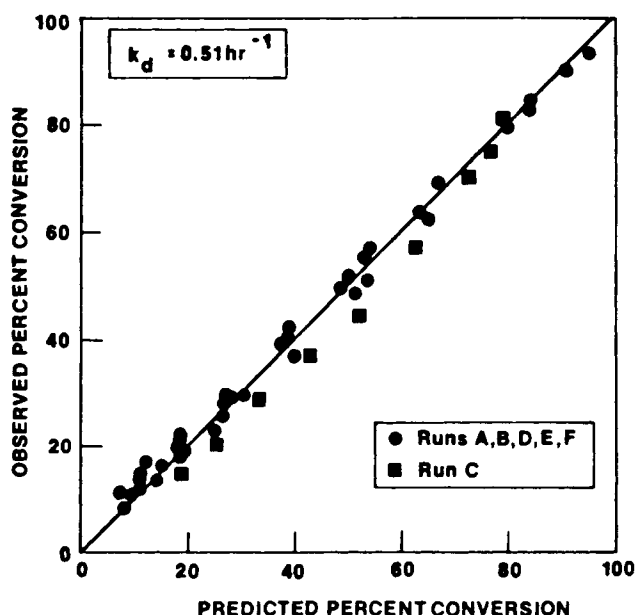


Figure 6. Agreement of theoretical deactivation model with experimental data (all runs).

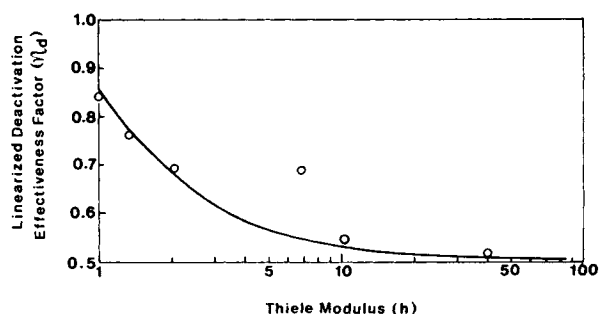


Figure 7. Dependence of linearized deactivation effectiveness factor on Thiele modulus: theory and experiment. $k_d = 0.51 \text{ h}^{-1}$ and $t_o = 2 \text{ h}$ in Eq. 9.

ment with the theoretical curve for $t_o = 2 \text{ h}$, and exhibit the same general trend predicted by theory. This general trend is particularly good for predicting the relationship between the slopes of Figure 3, since the Thiele modulus is seen to vary in these experiments between unity and 40, an exceedingly wide range. Again, the only significant deviant from the curve is the single experimental run already mentioned. The experimental reason for this deviation has not been determined.

Therefore, the data of Table 4 may be described either by the exact nonlinear theory of Eqs. 3 and 5 or by the linear approximation of Eqs. 8 and 9. This latter representation is intriguing because the term η_d appears to represent a time-invariant deactivation effectiveness factor with strong analogies to the effectiveness factor for nondeactivating first order reactions. Sufficient experience has not yet been accumulated to determine if the approach represented by Equations 8 and 9 can be generalized to other systems.

CONCLUDING REMARKS

The presence of internal diffusion can cause pseudo-deactivation rate constants, read directly as the slope from Levenspiel plots, to vary substantially from the intrinsic deactivation rate constant. Experimental data on peroxide decomposition by catalase exhibited substantial linearity of Levenspiel plots in the presence of the nonlinear effects of internal diffusion. Furthermore, these data verified the applicability of the nonlinear deactivation effectiveness factor theory, as well as suggesting the possible utility of the linear approximation thereto.

NOTATION

- A = deactivation time scale = $\exp(-k_d t / 2)$
- A_o = deactivation time scale at $t = t_o$
- a = fractional catalyst activity
- C_{Ar} = reactant concentration inside spherical particle, g mol/L
- D_A = effective diffusivity of reactant within spherical particle, cm^2/s
- E = activation energy for reaction, cal/g mole
- h = Thiele modulus, $= R/3 \sqrt{k_i/D_A}$
- k_i = intrinsic reaction rate constant, s^{-1}
- k = reaction rate constant, $= (k_i/\rho_p)$, $\text{cc}/(\text{s})(\text{g cat.})$
- k_p = pseudo reaction rate constant, $\text{cc}/(\text{s})(\text{g cat.})$
- k_d = deactivation rate constant, h^{-1}
- k_{dp} = pseudo deactivation rate constant, h^{-1}
- R = radius of spherical particle, cm
- r = radial position, cm
- t = process time, hours

- t_o = time about which Taylor expansion is made, hours
- x = conversion of reactant

Greek Letters

- η = isothermal effectiveness factor for hydrogen peroxide decomposition kinetics
- η_i = initialized effectiveness factor, given by Eq. 5
- η_d = deactivation effectiveness factor, given by Eq. 8
- ρ_p = density of catalyst particle, g/cc
- τ = space time, s (g cat.)/(cc)
- ϕ = deactivation modulus $= (3hA)$
- ϕ_o = deactivation modulus at $t = t_o$

LITERATURE CITED

- Altomare, R. E. et al., "Deactivation of Immobilized Beef Liver Catalase by Hydrogen Peroxide," *Biotech. Bioeng.*, **16**, 1659 (1974a).
- Altomare, R. E. et al., "Inactivation of Immobilized Fungal Catalase by Hydrogen Peroxide," *Biotech. Bioeng.*, **16**, 1675 (1974b).
- Balder, J. R., and E. E. Petersen, "Poisoning Studies in a Single Pellet Reactor," *Chem. Eng. Sci.*, **23**, 1287 (1968).
- Butt, J. B., S. D. Diaz and W. E. Muno, "Effects of Coking on the Transport Properties of H-Mordenite," *J. Catalysis*, **37**, 158 (1975).
- Chu, C., "Effect of Adsorption on the Fouling of Catalyst Pellets," *IEC Fund.*, **7**, 509 (1968).
- Hegedus, L. L., "On the Poisoning of Porous Catalysts by an Impurity in the Feed," *IEC Fund.*, **13**, 190 (1974).
- Hegedus, L. L., and E. E. Petersen, "Study of the Mechanism and Kinetics of Poisoning Phenomena in a Diffusion-Influenced Single Catalyst Pellet," *Chem. Eng. Sci.*, **28**, 69 (1973a).
- Hegedus, L. L., and E. E. Petersen, "Experimental Study of the Poisoning of a Single Catalyst Pellet in a Diffusion Reactor," *Chem. Eng. Sci.*, **28**, 345 (1973).
- Kittrell, J. R., "Mathematical Modeling of Chemical Reactions," *Adv. Chem. Eng.*, **8**, 97 (1970).
- Krishnaswamy, S., "Studies of Solid Catalyzed Systems Subject to Catalyst Deactivation and Diffusional Limitations," Ph.D. thesis, University of Massachusetts (1978).
- Krishnaswamy, S., and J. R. Kittrell, "Diffusion Influences on Deactivation Rates," *AIChE J.*, **27**, 120 (1981a).
- Krishnaswamy, S., and J. R. Kittrell, "The Effect of External Diffusion on Deactivation Rates," *AIChE J.*, **27**, 125 (1981b).
- Levenspiel, O., *Chemical Reaction Engineering, Second Edition*, John Wiley and Sons, Inc. (1972).
- Masamune, S., and J. M. Smith, "Performance of Fouled Catalyst Pellets," *AIChE J.*, **12**, 384 (1966).
- Ogunye, A. F., and W. H. Ray, "Optimal Control Policies for Tubular Reactors Experiencing Catalyst Decay," *AIChE J.*, **17**, 43 (1971).
- Olson, J. H., "Rates of Poisoning in Fixed-Bed Reactors," *IEC Fund.*, **7**, 509 (1968).
- Rovito, B. J., and J. R. Kittrell, "Film and Pore Diffusion Studies with Immobilized Glucose Oxidase," *Biotech. Bioeng.*, **15**, 143 (1973).
- Smith, J. M., *Chemical Engineering Kinetics, Second Edition*, McGraw Hill (1970).
- Strangeland, B. S., and J. R. Kittrell, "Jet Fuel Selectivity in Hydrocracking," *IEC Proc. Des. Dev.*, **11**, 15 (1972).
- Suga, K., Y. Morita, E. Kunagita and T. Otake, "Deterioration of Catalysts for the Dehydrogenation of n-Butane due to Diffusion in Particles," *Int. Chem. Eng.*, **7**, 742 (1967).
- Szepe, S., and O. Levenspiel, "Catalyst Deactivation," *Chem. Eng. Sci.*, **23**, 881 (1968).
- Weekman, V. W., and D. M. Nace, "Kinetics of Catalytic Cracking Selectivity in Fixed, Moving and Fluid Bed Reactors," *AIChE J.*, **16**, 397 (1970).
- Wheeler, A., "Catalysis," P. H. Emmet, ed., **II**, Reinhold, New York (1955).

Manuscript received April 21, 1978; revision received May 5, and accepted May 15, 1981